Preparation and High-Temperature CO_2 Capture Properties of Nanocrystalline Na_2ZrO_3

Tiejun Zhao, Esther Ochoa-Fernández, Magnus Rønning, and De Chen*

Department of Chemical Engineering, Norwegian University of Science and Technology, N-7491 Trondheim, Norway

Received November 16, 2006. Revised Manuscript Received March 12, 2007

A novel method for producing nanosized Na_2ZrO_3 with well-controlled crystal phase has been developed, resulting in excellent kinetics for CO_2 capture at high temperatures. The novel preparation method involves a soft-chemical route starting with the generation of a complex from zirconoxy nitrate and sodium citrate, followed by a strong exothermic reaction between nitrate and citrate during calcination in a controlled atmosphere. The in situ produced carbon during the calcination serves as a dispersant of the oxide, and subsequent carbon burnoff promotes the formation of nanocrystalline Na_2ZrO_3 with an open pore structure. The calcination temperature and atmosphere are very crucial for controlling the crystal phase of Na_2ZrO_3. The resulting sodium zirconate samples are characterized by XRD, N_2 adsorption, Hg porosimetry, and SEM. A two-step calcination at 1073 K results mainly in the monoclinic phase, whereas one-step calcination at 1073 K or higher enhances the formation of the thermodynamically stable phase, namely hexagonal Na_2ZrO_3. A kinetic study of CO_2 capture in a tapered element oscillating microbalance (TEOM) reactor has shown that the monoclinic Na_2ZrO_3 is much more active than its hexagonal counterpart. The ability to work at CO_2 partial pressures as low as 0.025 bar, together with the excellent stability in multicycle capture/regeneration makes nanocrystalline Na_2ZrO_3 a very promising CO_2 acceptor for different applications.

1. Introduction

CO_2 capture technologies are desirable in order to significantly reduce CO_2 emissions from fuel-fired power stations and hydrogen-production processes.[1] Sorption-enhanced steam methane reforming (SESMR) is a promising process for H_2 production of high purity (>95%) in one step, where CO_2 acceptors are installed with the reforming catalyst.[2,3] Alkali zirconates such as Li_2ZrO_3 and Na_2ZrO_3, have been referred to as effective CO_2 acceptors because of their reversible CO_2 capture/regeneration and suitable thermodynamic properties at certain temperatures.[4−8] Conventionally, these materials have been prepared by solid-state reactions at high temperatures, using zirconium oxide and alkali salts as precursors.[4−7] The resulting materials often present relatively large particles and poor purity, leading to limited capacity and kinetics for CO_2 capture.

High-purity nanocrystalline materials are expected to enhance the CO_2 capture/regeneration rates because of their improved characteristics, such as higher surface area and higher surface reactivity due to the unsaturated bonds on their pristine surfaces.[9−12] We have recently developed a simple soft-chemical route to prepare nanosized Li_2ZrO_3 using zirconoxy nitrate and lithium acetate as precursors. The key factor in this technique is a vigorous release of gases from the oxidation reaction between the nitrates and acetates during the calcination, which facilitates the formation of nanocrystalline lithium zirconate and reduces particle sintering.[13,14]

The CO_2 capture properties are strongly dependent on the structure of the resulting oxides. Because the CO_2-capture reaction is volume-increasing and often exothermic, such nanocrystalline materials with open pore structure and large pore volume are expected to promote the capture/regeneration rates of carbon dioxide and suppress sintering of the nanoparticles. In addition, from an engineering point of view for applications in sorption-enhanced steam methane reforming (SESMR), one of the main challenges is to develop

* Corresponding author. Tel: 47-7359-3149. Fax: 47-7359 5047. E-mail: chen@nt.ntnu.no.

(1) Rostrup-Nielsen, J. R. *Catal. Rev.* **2004**, *46*, 247.
(2) Lopez Ortiz, A.; Harrison, D. P. *Ind. Eng. Chem. Res.* **2001**, *40*, 5102.
(3) Xiu, G. H.; Soares, J. L.; Li, P.; Rodrigues, A. E. *AIChE J.* **2002**, *48*, 2817.
(4) Nair, B. N.; Yamaguchi, T.; Kawamura, H.; Nakao, S. I. *J. Am. Ceram. Soc.* **2004**, *87*, 68.
(5) Ida, J.; Lin, Y. S. *Environ. Sci. Technol.* **2003**, *37*, 1999.
(6) Reddy, H. P.; Smirniotis, P. G. *J. Phys. Chem. B* **2004**, *108*, 7794.
(7) López-Ortiz, A.; Perez Rivera, N. G.; Reyes Rojas, A; Lardizabal, G D. *Sep. Sci. Technol.* **2004**, *39*, 3559.
(8) Ochoa-Fernández, E.; Rønning, M.; Grande, T.; Chen, D. Norwegian Hydrogen Seminar, Kvitfjell, Norway, Nov 15−16, 2004; Research Council of Norway and The Gas Technology Center, The Norwegian University of Science and Technology and the Foundation for Scientific and Industrial Research: Olso, Norway, and Trondheim, Norway, 2004; http://h2seminar2004.ife.no.
(9) Cushing, B. L.; Kolesnichenko, V. L.; O'Connor, C. J. *Chem. Rev.* **2004**, *104*, 3893.
(10) Pfeiffer, H.; Bosch, P. *Chem. Mater.* **2005**, *17*, 1704−1710.
(11) Vasylkiv, O.; Sakka, Y. *Nano Lett.* **2005**, *5*, 2598.
(12) Feng, X.; Hu, M. Z. In *Encyclopedia of Nanoscience and Nanotechnology*, Nalwa, H. S., Ed.; American Scientific: Valenica, CA, 2004; Vol. 1, p 687.
(13) Ochoa-Fernández, E.; Rønning, M.; Grande, T.; Chen, D. *Chem. Mater.* **2006**, *18*, 1383.
(14) Ochoa-Fernández, E.; Rønning, M.; Grande, T.; Chen, D. *Chem. Mater.* **2006**, *18*, 6037.

10.1021/cm062732h CCC: $37.00
Published on Web 05/22/2007

efficient acceptors with fast kinetics, especially at low CO_2 partial pressures. This should be combined with high stability and high capacity at the working temperatures and the ability to easily be regenerated.[14]

It has been reported that there are several pathways to prepare nanosized multinary oxides.[9] Minimizing diffusion pathways by intimate mixing of the different metal precursors on an atomic scale or restricting the reaction space normally results in a decrease in the temperature necessary for the formation of the defined oxide phase, such as the sol−gel and the reverse micelles methods.[9] However, the above methods are typically multistep procedures and expensive reagents are often involved. Recently, Schwickardi et al. have reported the preparation of active carbon-mediated high-surface-area nanosized oxides.[15] During this process, a highly concentrated metal precursor solution is impregnated on active carbons and subsequently calcinated in order to burn off the carbon. The obtained oxides have high surface areas. In addition, carbon nanotubes have been used as templates for the synthesis of mesoporous zoelites.[16] In this study, a versatile and controllable soft-chemical-derived route for the synthesis of porous nanocrystalline Na_2ZrO_3 is developed. The technique relies on the strong exothermic reaction and in situ carbonation of the precursor complex, thus avoiding the extra addition of a carbon template during the synthesis. The CO_2 capture kinetics and durability of the Na_2ZrO_3 are investigated in an oscillating microbalance reactor (TEOM) at various CO_2 concentrations for defined capture/ regeneration temperatures.

2. Experimental Section

Sodium citrate (NaCA) and zirconoxy nitrate ($ZrO(NO_3)_2 \cdot xH_2O$) were dissolved in deionized water and mixed under vigorous agitation for 3 h. The Na/Zr molar ratios used for the synthesis of sodium zirconate was 2.0. The resulting solution was evaporated under continuous stirring at 363 K overnight, leading to the formation of an amorphous zirconium complex. Similar preparation details have been described elsewhere.[13,14] The obtained amorphous zirconium complex was then placed in an alumina crucible and heat-treated in a muffle oven with a defined temperature program and gas atmosphere. The effects of the calcination procedure and atmosphere have been studied, and five different samples were prepared.

Samples A and B: The amorphous zirconium complex was heated from room temperature to 673 K at a rate of 10 K/min under argon and air flow, respectively.

Sample C: The amorphous zirconium complex was treated from room temperature to 1073 K at 10K/min under an argon flow and then calcined at this temperature for 3 h in air. It is referred to as the two-step calcination procedure.

Sample D: The amorphous zirconium complex was heated from room temperature to 1073 K at a rate of 10 K/min in air and kept there for 3 h, which is referred to as one-step calcination.

Sample E: The amorphous zirconium complex was treated from room temperature to 1173 K at a rate of 10 K/min under an argon flow and then calcined at this temperature for 3 h in air.

Powder X-ray diffraction (XRD) measurements were performed in a Siemens D5005 (40 kV, 50 mA) X-ray diffractometer with Cu−Kα radiation (λ = 1.541 Å). The average crystal sizes of samples C−E were calculated using the Scherrer equation for the most intense peak in the diffraction patterns.

TGA-DTA analyses of the amorphous complex (30.0 mg) were carried out in a Netzsch STA-449C thermobalance to investigate the strong exothermic reaction process. Two calcination experiments were followed by TGA-DTA with exact conditions as samples A and B under a flow rate of 50 mL/min. The gases evolved during this analysis were monitored by a QMS mass spectrometer (Thermostar Pfeiffer Vacuum). In addition, to confirm the coke formation, we further calcined sample A at 673 K for 1 h in Ar.

Differential scanning calorimetry (DSC) was performed in a Perkin-Elmer DSC Diamond 7 instrument in an argon or air flow of 50 mL/min. The zirconium complex (50.0 mg) was loaded in aluminum pans, which were compressed, with holes remaining on the cover of the pans. Temperature-programmed experiments were carried out at a heating rate of 5 K/min from room temperature to 673K and kept at 673K for another 1 h.

N_2 adsorption isotherms were measured on a Micromeritics TriStar 3000 instrument at a liquid N_2 temperature, 77 K to determine the BET surface area and pore volume (2-300 nm) by the BJH method. Prior to the measurement, all the samples were degassed at 573 K overnight. The mesopore and macropore volumes (>100 nm) were also measured by mercury intrusion porosimetry in a Carlo Erba Porosimeter 2000. All the samples were evacuated and dried at 423 K prior to analysis. The obtained data were analyzed on the basis of the assumption of a cylinder pore model.

Electron micrographs were acquired using a SEM (JEOL JSM 3600LV) and a TEM (JEOL JEM 2100, operated at 200 kV). For the TEM samples, a suspension of small amounts of sample C in ethanol were given an ultrasonic treatment for 5 min and then dropped onto a copper grid covered by a holey carbon film.

CO_2 capture properties were evaluated using a tapered element oscillating microbalance (TEOM) as described earlier.[14,17] Typically, the tapered element, loaded with 20.0 mg of Na_2ZrO_3 sample diluted with quartz particles, was heated to 903 K at a heating rate of 10 K/min in pure Ar and kept for 60 min at these conditions in order to refresh the surface of the sample. Afterwards, the temperature was decreased to the selected temperature for CO_2 capture measurements: 848 K. The CO_2 capture was initiated by switching from Ar to a flow with a defined CO_2 partial pressure at the same temperature. The total flow rates of the Ar and CO_2 mixture were kept constant at 100 mL/min. After saturation of the acceptor, the temperature was increased at 10 K/min to 953 K, and the gas flow was changed from a CO_2/Ar mixture to the pure Ar to release the CO_2. The operating pressure is maintained at 1.0 bar.

3. Results and Discussion

Figure 1 shows the XRD patterns of the powders obtained after evaporation of the precursor solution and samples A, C, D, and E calcined at different conditions. Only diffraction lines of $NaNO_3$ can be observed in the case of the amorphous zirconium complex sample. XRD patterns of sample B are similar to that of sample A and not shown here. Characteristic peaks of tetragonal ZrO_2 are observed in sample A calcined at 673 K. Na_2ZrO_3 formation is observed in samples C−E calcined at 1073 K or higher, indicating that temperatures higher than 673 K are needed

(15) Schwickardi, M.; Johann, T.; Schmidt, W.; Schuth, F. *Chem. Mater.* **2002**, *14*, 3913.
(16) Schmidt, I.; Boisen, A.; Gustavsson, E.; Stahl, K.; Pehrson, S.; Dahl, S.; Carlsson, A.; Jacobsen, C. J. H. *Chem. Mater.* **2001**, *13*, 4416.
(17) Chen, D.; Rebo, H. P.; Moljord, K.; Holmen, A. *Chem. Eng. Sci.* **1996**, *51*, 2687.

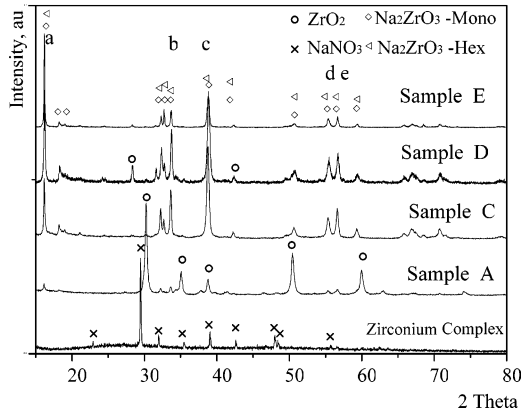

Figure 1. XRD diffraction patterns of the dried zirconium complex and the calcined sodium zirconate samples.

Table 1. Intensity Ratios of Diffraction Peaks on Different Samples of Sodium Zirconate[a]

samples	monoclinic	hexagonal	sample C	sample D	sample E
I_a/I_{max}	0.37	1.00	0.62	1.00	1.00
I_b/I_{max}	0.40	0.30	0.46	0.56	0.39
I_c/I_{max}	1.00	0.20	1.0	0.98	0.62
I_d/I_{max}	0.25	0.10	0.25	0.27	0.15
I_e/I_{max}	0.27	0.10	0.27	0.31	0.21

[a] I_i/I_{max} is defined as the intensity ratio of diffraction pattern at position i with the maximum for i = a−e. The positions of a−e are presented in Figure 1.

for the formation of Na_2ZrO_3. Moreover, by comparison with the peaks of samples C and D, a larger fraction of monoclinic ZrO_2 in sample D as shown in Figure 1 can probably be ascribed to prolonged exposure to oxygen, which promotes the formation of thermodynamically stable monoclinic ZrO_2 phase at a certain temperature range.[18,19] It seems that the oxygen might play a key role in the phase transformation of Na_2ZrO_3. However, a more detailed study on the effect of calcination conditions on the properties of Na_2ZrO_3 is in progress.

It is observed from Figure 1 that the crystalline structure of Na_2ZrO_3 is dependent on the calcination procedure and varies for the different samples. All the calcined samples show diffraction lines at almost identical 2θ values, but with different intensities. The different intensities of the diffraction peaks are probably ascribed to the transformation of the crystallographic phases. Furthermore, the analysis of the intensity ratio of the diffraction lines at different angles can help to determine the purity of Na_2ZrO_3. The two different crystallographic phases, namely, monoclinic and hexagonal, have characteristic ratios between the diffraction lines. These ratios for both monocline and hexagonal Na_2ZrO_3 (from the JCPDS database) together with the ratios calculated for the samples prepared in this study are collected in Table 1.

Thus, the crystalline structure of the prepared samples can be simply determined by comparison of these values with those of the model compounds. For example, the ratios obtained for sample C (I_b/I_{max} = 0.46; I_c/I_{max} = 1.0; I_d/I_{max} = 0.25; I_e/I_{max} = 0.27) are similar to the values observed for monoclinic Na_2ZrO_3 (I_b/I_{max} = 0.40; I_c/I_{max} = 1.0; I_d/I_{max} =0.25; I_e/I_{max}= 0.27). The only major difference is between the ratio I_a/I_{max}, 0.62 and 0.37, respectively. This can be related to the presence of a small fraction of hexagonal Na_2ZrO_3 (I_a/I_{max} = 1.00), 1.0 in sample C. It is thus confirmed that relatively pure monoclinic Na_2ZrO_3 is produced by the two-step calcination procedure (sample C). On the basis of a similar analysis of the data in Table 1, it can be concluded that mainly the hexagonal phase is formed at higher calcination temperatures (sample E). This shows that the monoclinic phase is transformed to the thermodynamically stable hexagonal phase with increasing temperatures. Furthermore, mixed monoclinic and hexagonal phase (sample D) can be obtained when the samples are treated directly under air from room temperature to 1073K, namely, one-step calcination, as shown in Figure 1. This confirms that the calcination atmosphere has a significant effect on the crystallographic phase of the final material. Previous reports by our group show that nanocrytalline lithium zirconates with tetragonal phase can be produced by calcination at 873 K in static air, whereas the monoclinic phase is produced at 1073 K.[13,14]

It should be noted that the values of the intensity ratios at positions b, d, and e on sample D are higher than the respective values for the monoclinic and hexagonal phase. This can be attributed to the fact that the maximum intensity at a position standardized as 1 in sample D is partially a contribution of the monoclinic phase, in which the value of I_a/I_{max} is only 0.37 at position a; therefore, the above higher values at positions b, d, and e reflect the facts that sample D contains both monoclinic and hexagonal phase.

The strong exothermic reaction process during calcination of the amorphous zirconium complex was characterized by TGA-DTA and DSC, as shown in panels a and b of Figure 2. The calcination conditions of samples A and B are reproduced. A slight weight loss was recorded during the initial period, which is due to the evaporation of remaining water or decomposition of citrate in the zirconium complex. A sudden weight change (more than 60%) together with a large heat release was observed at temperatures about 573 K in air and 593 K in argon, respectively.

Note that the zirconium complex powders, initially located in the alumina pan of the TGA, are partially blown out of the pan during the experiments because of the gas evolution. As a result, we can speculate that the DTA data obtained are probably influenced by the sample weight loss. Therefore, a separate experiment in DSC in an argon or air atmosphere was carried out using a semisealed aluminum pan. The results are shown in Figure 2b.

From Figure 2b, three different regions, namely, a−c and a′−c′, can be found during calcination in air or argon flow, respectively. It is observed that some heat flow is required in the initial period, region a in air and a′ in argon, probably due to the evaporation of water or decomposition of citrate, as stated before. Less heat flow is required in region b from 423 to 543 K in air, because of the exothermic reaction between oxygen/nitrate and citrate; similar observations can be found in region b′ between 523 and 563 K, as shown in Figure 2b in argon, indicating that the reaction between nitrate and citrate also takes place in this period. However,

(18) Srinivasan, R.; Davis, B. H.; Cavin, O. B.; Hubbard, C. R. *J. Am. Ceram. Soc.* **1992**, *75*, 1217.
(19) Stichert, W.; Schuth, F. *Chem. Mater.* **1998**, *10*, 2020.

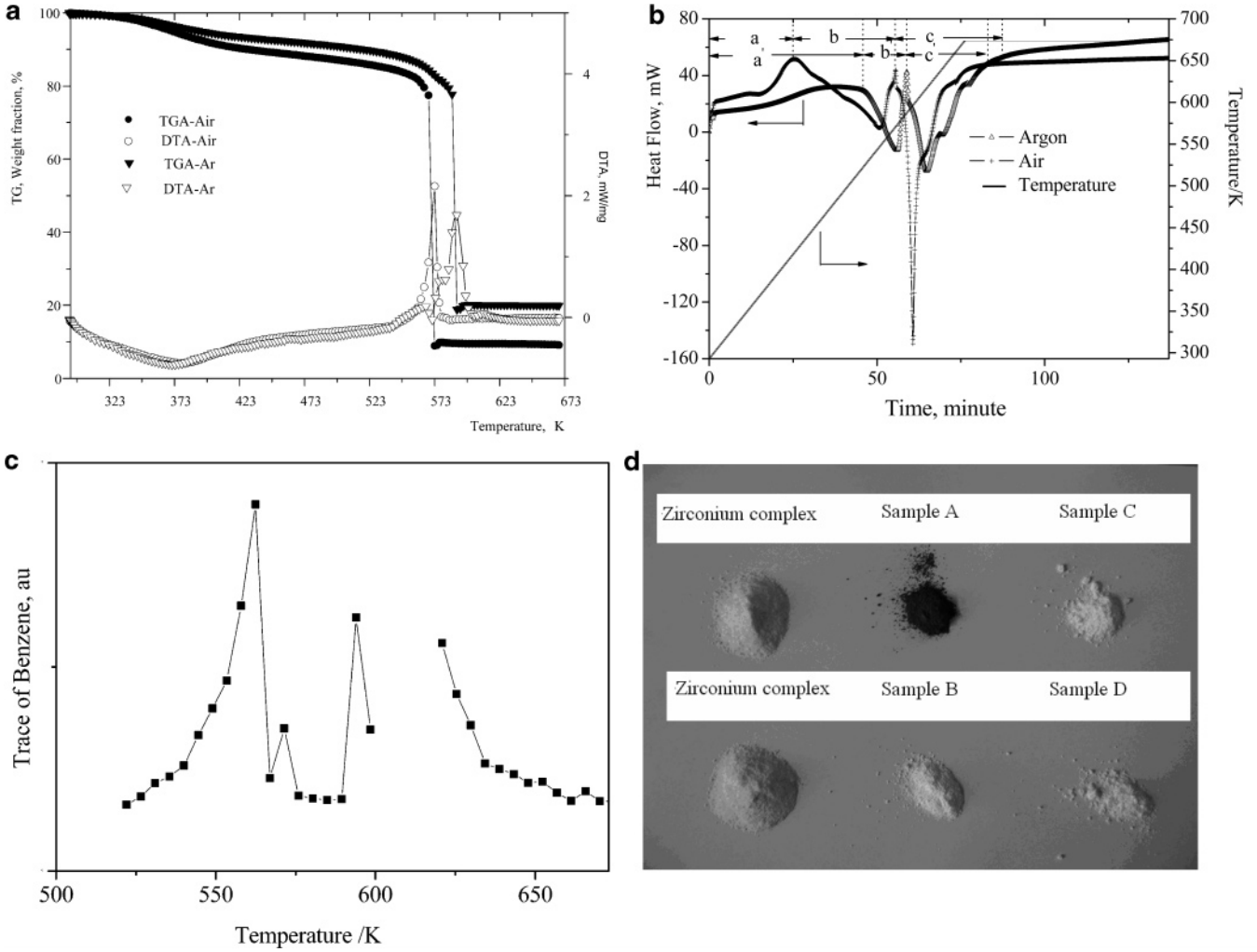

Figure 2. (a) TGA-DTA profiles of the amorphous zirconium complex in argon and air. Sample weight, 30 mg; gas flow rate, 50 mL/min; temperature ramp rate, 10 K/min to 673 K; (b) DSC curves of the zirconium complex in argon and air. Sample weight, 50 mg; gas flow, 50 mL/min; temperature ramp rate, 5 K/min to 673 K; (c) MS trace of benzene during the argon-annealing process; (d) images of the different prepared samples showing the carbon formation in argon flow during calcination.

the reaction in this period is rather mild. The increased heat flow required at the end of region b and b′ near 573 K is probably due to the partially melting of sodium nitrate, which has a melting point of 580 K. Furthermore, a sharp heat flow is released for the air-treated sample (region c), whereas a mild heat flow is released for the argon-treated sample (region c′). This heat release is certainly related to the strong exothermic reaction between the nitrates/oxygen and the citrates present in the precursor. We should point out that it is rather difficult to exactly estimate the heat released during the calcination, because multisteps involving both endothermic and exothermic processes are overlapped as shown in Figure 2b.

The gases evolved during calcination were followed by a coupled MS, and traces of benzene were found during calcination in argon as shown in Figure 2c. This indicates the formation of coke (carbon), which is considered responsible for the lower heat released in the argon flow. No obvious benzene signal is detected in the MS profile during calcination in an air flow. Moreover, formation of carbon was evident during calcination in Ar (sample A) due to the observed color change in the sample from white to black as shown in Figure 2d. A smoldering process during the calcination in argon flow is also observed. No such carbon formation was observed during calcinations in air (sample B). It should be noted that the rapid gaseous product released by the oxidation reaction between nitrate/oxygen and citrate limits interparticle contact, resulting in less sintering of the products.

Further morphology examination by SEM of sample C in Figure 3a shows that an open pore structure stacked by individual Na_2ZrO_3 is produced. In contrast, sample D has a less-porous structure with larger particles, as shown in Figure 3b. The in situ produced carbon in sample C acts as a dispersant during the calcination and yields an open structure with smaller particle size. During the calcinations in air (sample D), all the carbon contained in the precursor citrate is burned off at temperatures lower than 673 K. Therefore, severe sintering takes place during the subsequent higher-temperature annealing. This is also valid for sample E, which has undergone a calcination procedure similar to sample C, using Ar to promote the in situ formation of carbon. As observed in Figure 3c, an open structure is also characteristic of this sample despite the higher calcination temperature. Thus, controlling the calcination procedure is crucial for the pore structure of the final product. The size

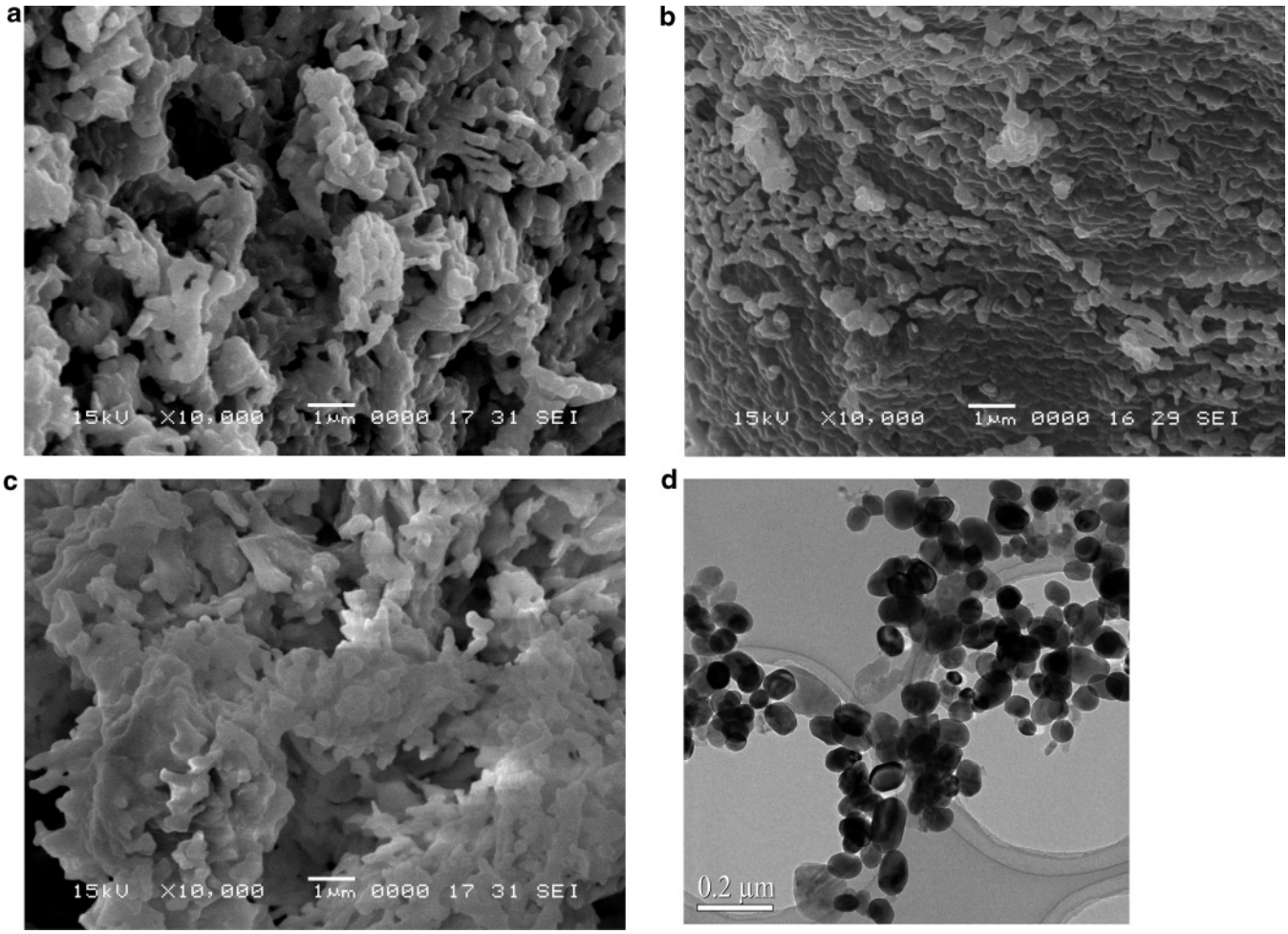

Figure 3. SEM and TEM images of Na_2ZrO_3 from different calcination procedures: (a) sample C, (b) sample D, (c) sample E, (d) size distribution of sample C.

Table 2. Textural Properties of Different Samples of Sodium Zirconate

samples	S_{BET} (m^2/g)	pore volume[a] (<300 nm) (cm^3/g)	pore volume[b] (>100 nm) (cm^3/g)	cryst size by XRD (nm)
C	5	0.031	0.82	30
D	4	0.028	0.33	41
E	4	0.016	0.75	59

distribution of the resulting Na_2ZrO_3 in sample C has been investigated by TEM. Spherical particles of diameter in the range 30−100 nm can be observed in the TEM image in Figure 3d. The crystallite sizes of samples C−E from different calcination procedures are also calculated using the Scherrer equation. The average particle size are 30, 41, and 59 nm, respectively, as shown in Table 2, indicating that the calcination procedure is also responsible for the different crystallite sizes of sodium zirconate.

The textural properties of Na_2ZrO_3 are listed in Table 2 and panels a and b of Figure 4. The reported BET surface areas of sample C−E are 5, 4, and 4 m^2/g, respectively. It seems that the preparation procedure does not lead to a significant change of the surface area of sodium zirconate. The obtained surface areas are in good agreement with the recent reported value (4 m^2/g) of sodium zirconate prepared by a precipitation method.[20]

Pore volumes determined both from N_2 physisorption (<300 nm) and Hg porosimetry (>100 nm) are shown in Table 2. By comparing the values in Table 2 and the isotherms in Figure 4a, it can be concluded that the micropore and mesopore volumes of all the samples produced from the above soft-chemical method are not very significant. However, the total pore volumes measured by Hg porosimetry are considerably higher and according to Figure 4b show a macropore size distribution. This indicates that the macropores dominate the porosity. The pores are formed from burning off the in situ produced carbons and the gas release by the reaction between citrate and nitrate. Furthermore, it is found that sample D has a lower porosity than samples C and E, which is in good agreement with the SEM images shown in Figure 3a−c. It has been reported that the existence of macropores would reduce the contact possibility of solid products after CO_2 capture, which is often considered as a major reason for the deactivation of acceptors such as calcium oxide.[21]

It can be concluded that the in situ produced carbon during calcination under an argon atmosphere, which is later burned in air flow, promotes the formation of mesoporous and macroporous structures and the dispersion of the nanocrystalline particles. Another advantage of this two-step calcination process compared to one-step calcination (using only air) is that the use of Ar reduces the heat released during

(20) Pfeiffer, H.; Lima, E.; Bosch, P. *Chem. Mater.* **2006**, *18*, 2642.
(21) Feng, B.; Liu, W.; Li, X.; An, H. *Energy Fuels* **2006**,*20*, 2417.

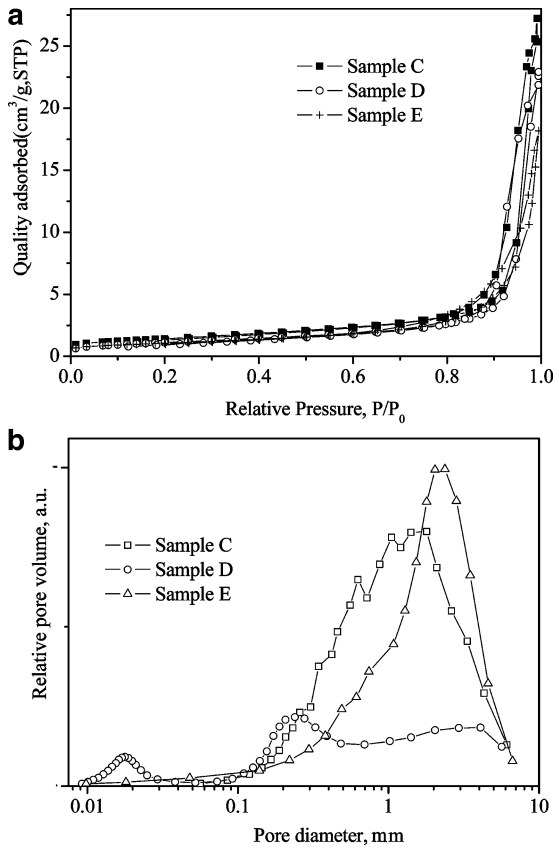

Figure 4. Textural properties of the Na_2ZrO_3 samples. (a) N_2 adsorption−desorption isotherms; (b) pore size distributions from Hg porosimetry.

the strong exothermic reaction, resulting in an improved phase purity of the final product. This is going to be crucial for the CO_2 capture kinetics of the resulting materials as discussed later. This simple preparation route represents several advantages compared to conventional active carbon or polymer template-burning methods.[11,22,23] The main difference is that this novel method yields the in situ carbon without the addition of extra carbon precursors. Thus, due to the strongly exothermic reaction between the precursors after complexation and no additional carbon sources, a minimum diffusion pathway can be achieved compared to the Penchini method.[9]

The CO_2 capture properties of the different prepared Na_2ZrO_3 samples at 848 K measured by TEOM are presented in Figure 5a. The partial pressure of CO_2 is set to 0.5 bar. All the samples have approximately the same capacity (about 17 wt %) for CO_2 capture; however, large differences are observed in the kinetic behavior. Sample C saturates in 60 s, whereas more than 2000 s are necessary for saturation of samples E and D under the same conditions. These results represent a large improvement compared to the kinetics reported on similar materials.[7] Na_2ZrO_3 prepared by solid-state reactions has earlier been proposed as a good candidate for CO_2 removal using pure CO_2 as a probe gas, where 10 min were needed for saturation compared to 60 s in our study in sample C. It is noted that the intermediate behavior for CO_2 capture on Sample D is found between samples C and E, as expected.

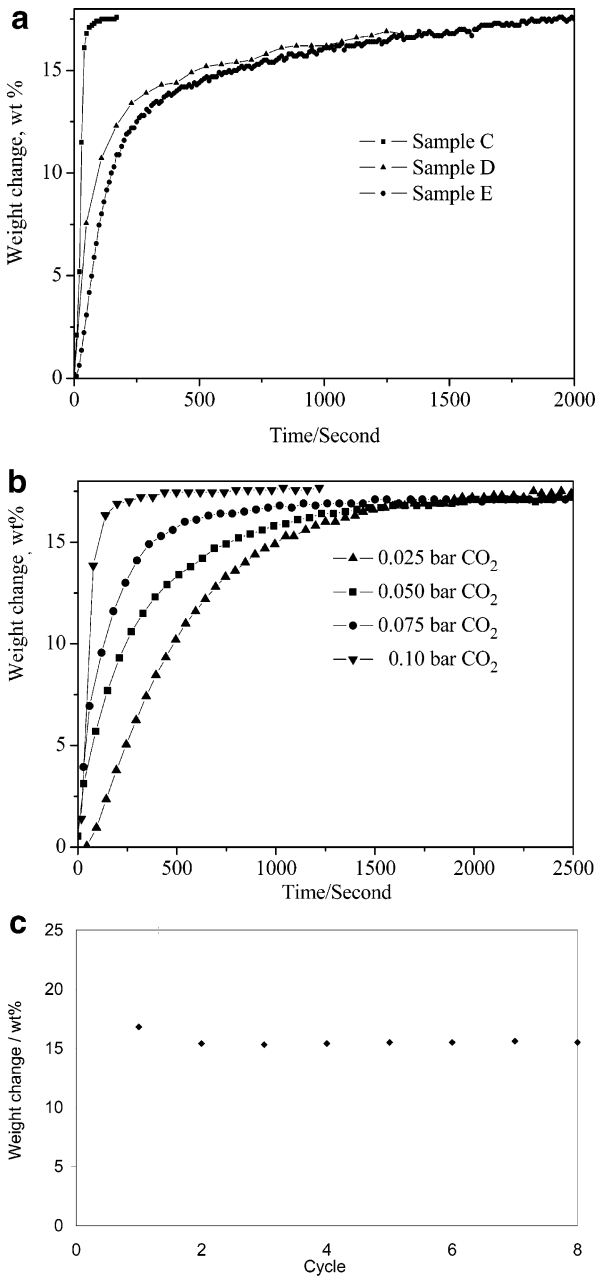

Figure 5. Carbon dioxide capture/regeneration properties for the sodium zirconate samples: (a) capture kinetics on Na_2ZrO_3 with different crystal phases, CO_2 partial pressure, 0.5 bar; (b) capture kinetics for sample C at different CO_2 partial pressures; (c) stability plot during eight cycles for sample C. Operating conditions: capture temperature, 848 K; regeneration temperature, 953 K; total flow rate, 100 mL/min; operating pressure, 1.0 atm.

The theoretical capacity of Na_2ZrO_3 on the basis of the weight of the acceptor is 23.8 wt %. However, ca. a 17 wt % increase can be observed during the TEOM test. The difference between the theoretical and real capacity for CO_2 capture is mostly likely due to the purity of the obtained Na_2ZrO_3. From the XRD patterns in Figure 1, the diffraction peaks of ZrO_2 are found; ZrO_2 does not react with CO_2 at the current operating conditions, thus lowering the CO_2 capture amounts. In addition, we cannot exclude the existence of amorphous Na_2CO_3 in all the samples, although no obvious characteristic peaks in XRD patterns are found.

(22) Martirosyan, K. S.; Luss, D. *AIChE J.* **2005**, *51*, 2081.

(23) Wohlrab, S.; Weiss, M.; Du, H.; Kaskel, S. *Chem. Mater.* **2006**, *18*, 4227.

Furthermore, the lower CO_2 capacity of Na_2ZrO_3 is also probably due to the relatively short time on stream in CO_2 flow. We can find the capacity in all the samples is still increasing even at 2000 s on stream, as shown in Figure 5a. According to the general principle of gas−solid reactions, the formation of a layered product (ZrO_2 and Na_2CO_3) would probably increase the diffusion barrier of CO_2 molecules through these layers; therefore, the capture rate becomes very slow at high degree of reaction. It should be pointed out that the capacity of acceptors in the initial periods with fast CO_2 capture rates is a crucial parameter for the applications in SESMR.

Generally, the CO_2 capture kinetics is related to the physicochemical properties of Na_2ZrO_3, such as the BET surface area, the pore size distribution, and the surface reactivity at the operating conditions. As discussed above, all the samples have very similar BET surface areas; therefore, this cannot explain the large differences observed in the capture rates. Combining the observations in Figure 5a that samples C and E have similar pore volumes but different CO_2 capture rates and that sample D shows a higher capture rate than sample E, although it has a lower pore volume as shown in Table 2, the pore volume seems to not be responsible for the different CO_2 capture rates in these samples. It should be pointed out that this conclusion is specific, because we deliberately design the preparation method to obtain the acceptors with higher pore volume and mainly focus on the kinetic behavior in the initial periods on stream. It is well-known that the role of the textural properties is very crucial under some specific conditions where the formation of solid products after CO_2 capture also increases the possibility of pore volume blockage.[21,24]

It should be noted that the CO_2 capture rates are significantly different in the initial periods and decrease with a decrease in the amount of monoclinic phase in these three samples. Therefore, monoclinic Na_2ZrO_3 is more active than the hexagonal phase because of the higher surface reactivity of the monoclinic phase. It can be concluded that the CO_2 capture rate is mostly determined by the surface reactivity of the respective substances. The importance of controlling the crystalline phase in order to optimize the capture properties was demonstrated in an earlier report for lithium zirconate.[13,14] Crystal size is another possible factor determining the CO_2 capture rate according to the results by XRD analysis as presented in Table 2: A higher CO_2 capture rate is obtained on the sample having smaller crystal size. It is difficult to separate the effect from the crystal size and the structure to some extent, because the hexagonal phase of Na_2ZrO_3 is often accompanied by a large crystal size due to the higher temperature treatments.

From Figure 5b, the uptake profiles of CO_2 capture for monoclinic Na_2ZrO_3 (sample C) at different partial pressures of CO_2 can be observed. It should be commented that samples E and D showed a poor behavior (less than 10 wt % capacity in 2500 s) under the same operating conditions at 0.1 bar CO_2. This is in agreement with the previous point that the surface reactivity of obtained monoclinic Na_2ZrO_3 samples plays a key role in the reaction with CO_2. However, only 5 min are needed to reach a capacity of about 17 wt % on the acceptors with dominating monoclinic Na_2ZrO_3 at 0.1 bar CO_2, and the acceptor works properly even under 0.025 bar of CO_2. The CO_2 capture rate decreases with the CO_2 partial pressure, as expected. We also have reported that the CO_2 capture rate is very slow on the nanocrystallite Li_2ZrO_3 at 0.1 bar CO_2.[14] This indicates that the CO_2 capture rates are strongly dependent on the surface reactivity of acceptors. It should be emphasized that the behavior of the acceptor at low CO_2 partial pressure is the most significant for the practical utilization of the material in processes such as SESMR.[25,26]

In addition to favorable kinetics, monoclinic Na_2ZrO_3 shows a promising stability in a multicycle study, as shown in Figure 5c, implying that no obvious crystal phase transformation occurs. However, the acceptor cannot be completely regenerated at the working conditions because of the limitation in the TEOM operating temperature (953 K), and the typical degree of the regeneration is around 80%. It was reported that the regeneration of Na_2ZrO_3 prepared by solid-state reaction started to occur only at temperatures higher than 1073 K under similar operation conditions.[7] The present work presents a significant improvement of the regeneration kinetics. However, from a thermodynamic point of view, higher temperature might be needed to regenerate the acceptors in the presence of a high partial percent of CO_2. Thus, possible deactivation of the solid acceptors due to phase transformation at higher temperatures should be addressed in future studies.

4. Conclusions

Controlled nanosized Na_2ZrO_3 has been synthesized by a novel soft-chemical route and it has been demonstrated as an effective CO_2 acceptor showing high capture rates at low CO_2 partial pressures. The strong exothermic reaction between nitrate and citrate not only promotes the in situ carbon formation, but also prevents formation of large particles by the dispersive role of the released gases. The in situ produced carbon promotes the pore formation and dispersion of the particles during the high-temperature annealing.

The porous monoclinic Na_2ZrO_3 is obtained by a two-step calcination procedure at 1073 K in Ar flow, followed by calcination in air flow during the heating. In contrast, a more densely stacked Na_2ZrO_3 with mixed monoclinic and hexagonal phase is obtained by one-step calcination in an air atmosphere, where almost no carbon residue remains at temperatures higher than 673 K. The porous structure and pore size distribution is obtained by SEM, N_2 adsorption, and Hg porosimetry. The particle size distribution of the

(24) Alvarez D.; Abanades J. C. *Energy Fuels* **2005**, *19*, 270.

(25) Ochoa- Fernández, E.; Rusten, H. K.; Jakobsen, H. A.; Rønning, M.; Holmen, A.; Chen, D. *Catal. Today* **2005**, *106*, 41.

(26) Ochoa-Fernández, E.; Haugen, G.; Zhao, T.; Rønning, M.; Aartun, I.; Børresen, B.; Rytter, E.; Rønnekleiv, M.; Chen, D. Process design simulation of H_2 production by sorption enhanced steam methane reforming: evaluation of potential CO_2 acceptors. *Green Chem.* **2007**, DOI: 10.1039/b614270b.

obtained monoclinic Na_2ZrO_3 is from 30 to 100 nm from the TEM image.

CO_2 capture studies of these synthesized Na_2ZrO_3 have been carried out in a TEOM at 848 K. It is found that much faster CO_2 capture rates can be obtained on the monoclinic Na_2ZrO_3 than that on the hexagonal one, even at low CO_2 partial pressures (0.025 bar). Stable CO_2 capture/regeneration behavior on monoclinic Na_2ZrO_3 is also observed.

In summary, a simple route for the formation of nanosized metal oxides with well-defined crystal phase due to in situ produced carbon formation to disperse the particles and to promote the porous structure formation has been developed. This route may be a promising platform to synthesize oxide materials for selected applications.

Acknowledgment. Support from the Research Council of Norway is greatly acknowledged.

CM062732H